Polymers **2014**, *6*, 2065-2081; doi:10.3390/polym6072065

OPEN ACCESS

polymers

ISSN 2073-4360

www.mdpi.com/journal/polymers

Article

Long-Term Bending Creep Behavior of Thin-Walled CFRP Tendon Pretensioned Spun Concrete Poles

Giovanni P. Terrasi [1,*], Urs Meier [2] and Christian Affolter [3]

[1] Head of the Mechanical Systems Engineering Laboratory of EMPA, Swiss Federal Laboratories for Materials Science and Technology, Überlandstrasse 129, CH-8600 Dübendorf, Switzerland

[2] Professor, Dr. h.c. and former Director of EMPA; Swiss Federal Laboratories for Materials Science and Technology, Überlandstrasse 129, CH-8600 Dübendorf, Switzerland; E-Mail: urs.meier@empa.ch

[3] Mechanical Systems Engineering Laboratory, EMPA; Swiss Federal Laboratories for Materials Science and Technology, Überlandstrasse 129, CH-8600 Dübendorf, Switzerland; E-Mail: christian.affolter@empa.ch

* Author to whom correspondence should be addressed; E-Mail: giovanni.terrasi@empa.ch; Tel.: +41-587-654-117; Fax: +41-587-654-010.

Received: 5 May 2014; in revised form: 3 July 2014 / Accepted: 16 July 2014 / Published: 23 July 2014

Abstract: This paper discusses the long-term behavior of a series of highly-loaded, spun concrete pole specimens prestressed with carbon fiber-reinforced polymer (CFRP) tendons, which were subjected to outdoor four-point bending creep tests since 1996 in the frame of collaboration with the Swiss precast concrete producer, SACAC (Società Anonima Cementi Armati Centrifugati). The 2 m span cylindrical beams studied are models for lighting poles produced for the last 10 years and sold on the European market. Five thin-walled pole specimens were investigated (diameter: 100 mm; wall-thickness: 25–27 mm). All specimens were produced in a pretensioning and spinning technique and were prestressed by pultruded CFRP tendons. Initially, two reference pole specimens were tested in quasi-static four-point bending to determine the short-term failure moment and to model the short-term flexural behavior. Then, three pole specimens were loaded to different bending creep moments: while the lowest loaded specimen was initially uncracked, the second specimen was loaded with 50% of the short-term bending failure moment and exhibited cracking immediately after load introduction. The highest loaded pole specimen sustained a bending moment of 72% of the short-term bending failure moment for 16.5 years before failing in July 2013, due to the bond failure of the tendons,

which led to local crushing of the high-performance spun concrete (HPSC). Besides this, long-term monitoring of the creep tests has shown a limited time- and temperature-dependent increase of the deflections over the years, mainly due to the creep of the concrete. A concrete creep-based model allowed for the calculation of the long-term bending curvatures with reasonable accuracy. Furthermore, the pole specimens showed crack patterns that were stable over time and minimal slippage of the tendons with respect to the pole's end-faces for the two lower load levels. The latter proves the successful and durable anchorage of these novel CFRP prestressing tendons in thin-walled, precast concrete members under realistic long-term service loads.

Keywords: carbon fiber-reinforced polymer; precast concrete; prestressed concrete; creep behavior; concrete poles

1. Introduction

When composites were introduced in structural engineering in the late 1970s, they were mainly applied as externally-bonded plate reinforcements or as post-tensioning elements replacing standard steel strands. Only one decade later, pultruded bars and tendons made of aramid, glass or carbon fiber-reinforced composites (AFRP, GFRP or CFRP, respectively) were first applied as prestressing elements in concrete beams [1–5]. Nanni and Tanigaki [6] presented one of the first experimental studies with aramid-reinforced tendons in prestressed concrete (PC) beams, where the development length was determined by varying the load span in bending experiments. Terrasi *et al.* [7] adopted the technique to hollow columns and pylons produced in pretensioned, spun concrete, where no external anchorage was required. The load transfer from the prestressing FRP tendon to the concrete was directly realized over the shear stresses in the interface FRP-concrete. In general, for prestressed systems without external anchorage, bond was either achieved over an uneven or corrugated tendon surface or over an additional sand coating ([8] provides a current overview). Sayed-Ahmad *et al.* [9] recently looked at the static bond performance of CFRP tendons embedded directly in concrete and demonstrated a 15% better bond for the sand-coated tendons compared to smooth ones.

Early experimental studies focused on the static mechanical performance of either the anchorage area of the prestressing elements, which was realized with mechanical anchors for post-tensioning systems [10–12], or on the static direct bond performance of tendons and rebars [13–16]. Static testing, however, cannot assess the degradation due to creep, which is a major cause for failure in the long term. Creep as a time-dependent failure mechanism could either occur due to stress relaxation in the prestressed FRP element itself [17] or due to creep in the interface between the bar and concrete [18].

Though GFRP is more susceptible to stress corrosion than composites with carbon fibers, there exist many developments and studies incorporating pretensioned concrete slabs and beams with GFRP tendons. Fornůsek *et al.* [19] presented a study about the long-term performance of concrete structures reinforced with prestressed GFRP tendons. They showed a considerable prestress loss of approximately 10% in the GFRP tendons within the first 132 days of the study. Terrasi *et al.* [20] recently reported on longer term CFRP prestress losses for a 27 m high electricity pole made of spun

concrete after five years of service. Prestress monitoring of eight CFRP tendons based on CFRP electric resistance measurements in the area of the fixture of the pole showed losses of 7% of the initial prestress (set to 1250 MPa) after five years, which correspond to the losses estimated on the basis of concrete compression creep and shrinkage experiments. The 40 pultruded CFRP tendons had a diameter of 5 mm and a quartz sand surface coating to enhance the bond to the high strength spun concrete of strength class C120 [7].

Already in 2003, Zou [21] presented an experimental work on beams prestressed with CFRP tendons. This is the only study comparable to the work presented in this paper and describes the long-term deformation and cracking behavior of beams prestressed with CFRP tendons over a period limited to 520 days. A performance comparable to beams prestressed with common steel strands was proven, and the high influence of the concrete strength on crack widths and creep deflections was shown. Zou and Shang [22] subsequently presented an analytical model for pretensioned beams and analyzed their model on three exemplary beam sections. Despite the lack of sufficient experimental long-term data with the creep of concrete structures incorporating composite reinforcement bars or tendons, many analytical approaches for the prediction of the creep behavior were developed. Mainly, the stress relaxation in the concrete was taken into account. Youakim and Karbhari [23] analyzed the prestress loss in pretensioned girders and compared the resulting long-term camber of the girder for different materials of the prestressing strands. Rodriguez-Gutierrez and Aristizabal-Ochoa [24] developed a similar model and validated it with measurements on posttensioned I-beams. Over-all, the cited experimental studies had a maximum duration of two years and were generally not able to produce any total failures of the prestressed structure, due to long-term effects in the material system; therefore, they were limited to report deflections, crack lengths and widths over time.

When the present authors started their research on the prestressing of slender spun concrete structures with carbon tendons [25], including all of the different challenges, such as temporary anchorage systems for prestressing, load transfer in the tendon-concrete interface and static and fatigue strength [26,27], the durability and creep resistance of such structures was an early and major concern, too [7]. Creep test data were already available for the individual components, such as the unidirectional pultrusion profiles or the epoxy and adhesives, but long-term data for the pole as a structural element with its new material combination were still missing. Therefore, the authors started a unique and still ongoing experiment with prestressed poles under permanent bending load for 17 years now. The goal of the study was the proof of the long-term stability of the poles, even under elevated loads, with a setup able to expose all different kinds of time-dependent failure mechanisms (stress relaxation in the tendons, bond failure, stress corrosion, concrete creep). The chosen load levels were 36%, 50% and 72% of the short-term failure moment of the same pole type tested in an identical four-point bending arrangement. The first total failure of a pole after 16.5 years proved the plausibility of the applied load levels in order to show the limits given by the bond strength between sand-coated CFRP-tendons and concrete.

2. Materials

The structural elements in the current study were CFRP prestressed hollow concrete cylinders. CFRP prestressing tendons of 3.0 mm in diameter, pultruded and sand-coated were used [25]. The

carbon fiber used was T700S by Toray (Tokyo, Japan) with a volume fraction of 72%, and the tendons had an epoxy polymer resin matrix with a glass transition temperature, T_g, of 110 °C. The tendons' average experimental tensile strength was 3375 MPa with a longitudinal elastic modulus E_{11} of 180.7 GPa and an average ultimate strain ε_{11u} of 1.87%. One should note that the carbon fiber T700S has a guaranteed ultimate tensile strain of 2.1%, which could not be reached in tensile testing, due to premature anchorage failure. In order to increase the bond to the concrete, the tendons' surface was roughened by coating it with a layer of epoxy (type Scotch Weld 2216 by 3M (St. Paul, MN, USA); average layer thickness: 0.25 mm), including hard aluminum oxide (Al_2O_3) sand granules of 0.5 mm in diameter. Additionally, a novel kind of shear reinforcement was used for the poles consisting of a CFRP tape spiral with polyamide matrix of pitch of 40 mm and a cross-section of 7 mm × 0.3 mm [25] (Figure 1). The low density, excellent stress-corrosion resistance and low creep and relaxation of CFRP are well known [28]. The above properties make unidirectional CFRP tendons particularly suitable as prestressing reinforcements for concrete elements [29].

Figure 1. Cross-section of carbon fiber-reinforced polymer (CFRP) prestressed pole specimens and the bending load arrangement.

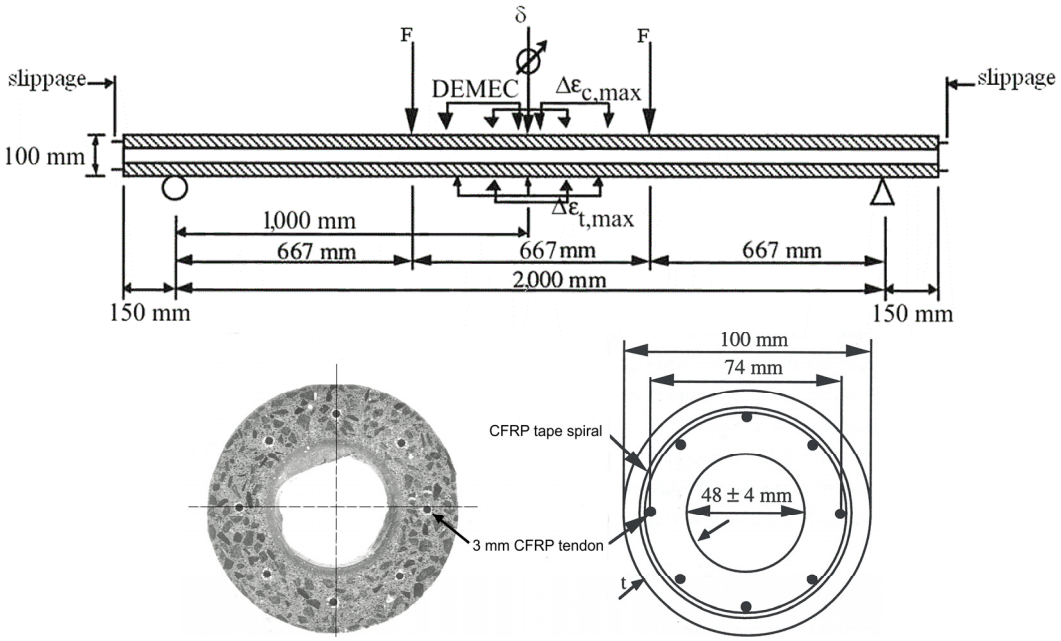

The current study used a high performance, centrifugally-cast concrete (high performance spun concrete (HPSC)) of strength class C115 (with a minimum 150 mm cube strength of 115 MPa after 28 days); this material is used for producing slender precast, prestressed poles and pylons in Switzerland [30]. The HPSC is characterized by a precise grain size distribution of selected 0–6 mm quartz sand aggregates, with a cement content of 600 kg·m^{-3} (of type CEM I 52.5 R). Silica fume (54 kg·m^{-3} were mixed into the concrete) and high performance superplasticizer (type Sika® ViscoCrete-20 HE® (Baar, Switzerland) at a content of 30 kg·m^{-3}) were important to achieve a high strength and a good flowability for the spinning process. This particular HPSC mix design allows for optimum spinning of hollow cylinders at water/(cement + silica fume) ratios in the range of 0.31–0.32. 20 mm long polypropylene (PP) fibers were included in the concrete mix at 1 kg·m^{-3} with the

objective of preventing shrinkage cracking. Concrete compaction was carried out by centrifugal casting for 15 min with a maximum revolution speed of 800 rpm in a pretensioning-spinning mold [25]. Prestress was released after 2 days, and then, the elements were demolded. The pole specimens were then kept in a 20 °C/90% R.H. (relative humidity) chamber for 7 days and, thereafter, left to cure under indoor ambient conditions.

The combination of CFRP and HPSC, along with an appropriate interface between them (sand-coating of the CFRP tendons), make it possible to minimize the weight of prestressed pole elements by reducing concrete cover and wall thickness while providing excellent serviceability (no susceptibility to corrosion, high bending stiffness [31] and high fatigue strength [27]). However, the performance of these elements under long-term bending was unknown at the time this investigation started (1996).

3. Experimental Specimens and Bending Test Setup

Five thin-walled (25–27 mm total thickness) 2.3 m-long cylindrical specimens (poles) with an outer diameter of 100 mm were centrifugally cast by precaster SACAC AG in Lenzburg, Switzerland (Figure 1). These identical poles were denominated No. 7, No. 8, No. 12, No. 13 and No. 14 (Table 1). Their cross-section dimensions correspond to the smallest lighting pole cross-section produced by SACAC for the European market [31]. The eight CFRP tendons per pole were stressed to an initial prestress of 1600 MPa, leading to a central HPSC prestress of 12.5 MPa after 28 days: The CFRP prestress was not monitored after demolding, but the prestress losses were analytically estimated to be 16.8% after 28 days from centrifugation [32]. This was calculated considering the experimentally determined E-modulus for the HPSC after two days from production (30 GPa), the measured shrinkage strain of the concrete (0.7‰ after 28 days) and the experimentally determined creep coefficient (0.62) of the concrete under similar central compression at 20 °C and 70% R.H. The tendons were evenly distributed on a circle with a diameter of 74 mm, had a cover of 11 mm and a tendon-to-tendon clear distance of 25 mm (Figure 1). Three DEMEC sensors (DEmountable MEChanical strain gauges) were placed on the tensile and compressive edge in the center-span (basic length: 200 mm; accuracy of strain measurement: ±0.01%), while the midspan deflection δ was measured with a LVDT (Linear Variable Differential Transducer) in the quasi-static bending tests and by a mechanical gauge in the bending creep tests (both with an accuracy of ±0.02 mm). The slippage of the top and bottom CFRP tendon (next to the compressive and tensile edge, respectively) was monitored at the poles' end surfaces with the aid of a sliding caliper (accuracy ±0.1 mm). Crack positions and crack widths were recorded during the tests with the aid of a crack microscope with an accuracy of ±0.02 mm, which was applied on the pole surface 20 mm under the horizontal axis of symmetry of the cylinder.

Poles Nos. 7 and 8 were tested in quasi static four-point bending at the age of 28 days, with lever arms of 667 mm, a span of 2000 mm and 150 mm of overhang on each end (Figure 1), while the creep tests with pole Nos. 12–14 were started at the age 28 days with the same span and load arrangement in outdoor four-point bending creep tests (Figure 2).

In the outdoor bending creep experiments, concrete blocks of known mass were hung in the two third-points of the pole specimens. Lead plates fixed thereon allowed the precise adjustment of the selected load level, taking into account the mass of the steel loading devices (Figure 2). Pole No. 12

was loaded with a constant bending moment of 2.07 kNm, which is just below the short-term cracking moments measured in the flexural test of pole No. 7 and pole No. 8 (2.41–2.58 kNm, Table 1). The bending creep moment of pole No. 13 (2.8 kNm) corresponded to the maximum short-term service moment of a five-meter high lighting pole under wind load [33] and was just above the short-term cracking moment. The highest loaded specimen, pole No. 14, was loaded (considering self-weight) with a bending moment of 72% of the average short-term failure moment ($M_{R,exp}$) determined in the flexural tests of poles Nos. 7 and 8 (5.645 kNm, Table 1).

Figure 2. Outdoor bending creep test of the highest loaded pole specimen (pole No. 14).

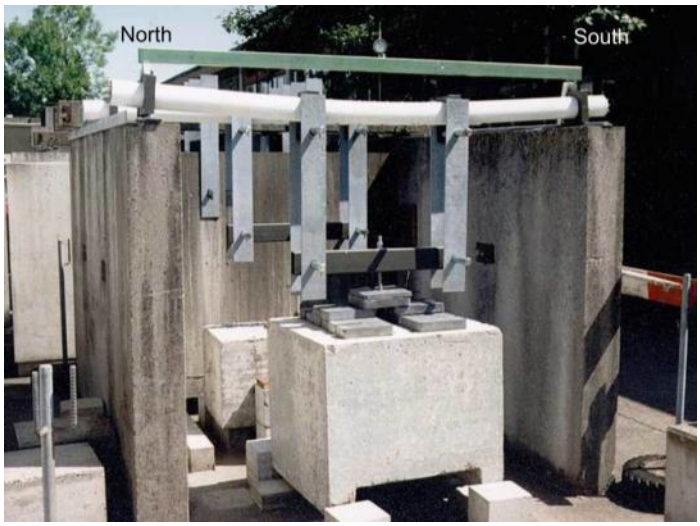

Table 1. Experimental program and main test results (n.a. means "not applicable", the maximum deflection and maximum strain values for pole No. 14 were last taken 1.4 years before failure *). HPSC, high-performance spun concrete.

Pole No.	Initial CFRP prestress (MPa)	Bending test	Cracking moment (kNm)	Creep moment (kNm)	Failure moment (kNm)	Time to failure	Midspan deflection at failure (mm)	$\Delta\varepsilon_{c,max}$ (‰)	$\Delta\varepsilon_{CFRP,max}$ (‰)	Failure mode
7	1600	quasi-static	2.58	n.a.	**5.76**	1 h	66.4	−5.37	10.55	HPSC crushing
8	1600	quasi-static	2.41	n.a.	**5.53**	1 h	70.6	−5.90	11.33	HPSC crushing
12	1600	creep	2.07	**2.07**	none	running	n.a.	−2.37	1.55	none
13	1600	creep	n.a.	**2.80**	none	running	n.a.	−4.14	3.92	none
14	1600	creep	n.a.	**4.07**	**4.07**	**16.54 y**	68.6 *	−6.84 *	9.27 *	bond

4. Results and Discussion

Table 1 shows the main test results of the two short-term bending tests to failure of the reference poles Nos. 7 and 8 and of pole Nos. 12–14 tested in bending creep. Unfortunately, the maximum creep deflection and maximum creep strain values for pole No. 14 were last taken 1.4 years before failure. Furthermore, the maximum bending strain $\Delta\varepsilon_{CFRP,max}$ of the outermost CFRP tendon (near the tensile

edge of the pole) is not measured directly, but can be calculated from the measured values of the maximum compression strain at the top edge of the pole $\Delta\varepsilon_{c,max}$ and the maximum tensile strain at the lower edge $\Delta\varepsilon_{t,max}$ (which were both determined by measuring strains over DEMEC gauges with a base length of 200 mm). In this case, the assumption is that "plane sections remain plane" during loading, which was experimentally proven in [25] to be a valid assumption for the short-term bending behavior. One should note that for the long-term bending behavior, this assumption is still valid [21] and that the tensile creep of the unidirectional CFRP tendons is very limited, even at high tensile stress levels [32,34], while the creep of the tendon surface bond layer is also rather limited in the central (cracked) span of the poles, due to the limited bond stresses present between the cracks [18,25]. Table 1 shows the high values $\Delta\varepsilon_{CFRP,max}$ of the outermost (lowest) CFRP tendons in the quasi-static bending tests to failure (around 11‰), which demonstrate that the outermost tendon reaches considerable tensile stresses if one takes into account that the tendon strain resulting from prestress after 28 days is 7.3‰ (considering prestress losses after [25,32]).

Figure 3. Quasi-static bending behavior of CFRP prestressed HPSC pole No. 7: Comparison of measured with calculated moment *vs.* curvature relationships.

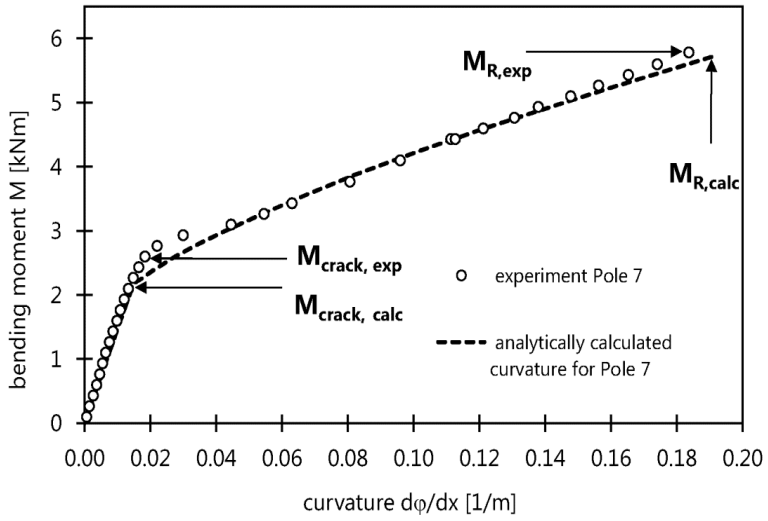

4.1. Short-Term Bending Behavior

Poles Nos. 7 and 8 showed an approximately bilinear load-deflection behavior with considerable deflection until failure that was caused by crushing of the HPSC compression zone. The crushing strains of the HPSC are remarkably high and reached an average value of 6‰ (see the values of $\Delta\varepsilon_{c,max}$ in Table 1, on top of which, the initial concrete strain due to prestress of 0.36‰ has to be added). Figure 3 shows the experimental moment *vs.* curvature diagram for pole No. 7, with the curvatures in the zone of pure bending derived from the strain measurements (DEMEC gauges) on the top and bottom edges during flexure. In the lower part of the diagram, the pole remained uncracked until the bending stresses overcame the centric prestress and the tensile strength of the HPSC (which was determined to be 10.9 ± 1.3 MPa in standard three-point bending tests of unreinforced spun cylinders of an age of 28 days). The kink in the moment-curvature curve was caused by the formation of the first bending cracks in the tensile zone of the central pole span. With the load increasing, the number of

cracks in the central span increased, and the cracked zone developed from the central span to the shear spans. Therefore, the curvature (and deflection) increased considerably. Figure 4 shows a state of increased deflection for the test of pole No. 8 at 98% of the failure load.

The experimental curvatures can be compared with analytically calculated results, which are shown in Figure 3 for pole No. 7. The theoretical calculation of the curvatures in the uncracked state is straightforward and requires determining the ideal moment of inertia of the full cross-section and the consideration of the elastic modulus of the HPSC, which is approximately 35 GPa [25].

In the cracked state, the bending curvature calculation requires a direct cross-sectional analysis: a value of the compressive strain on the top flange is assumed, which, under consideration of the prestress, defines the strain distribution in the HPSC and in the CFRP tendons over the section. In particular, in [25], a bond coefficient of 0.95 according to [35] is considered. This value was estimated at failure and gives an upper limit for the bond coefficient of the sand-coated CFRP tendons to the HPSC, which leads to a slight overestimation of the curvatures at lower load levels (just after cracking, Figure 3). Knowing the strain distribution in the HPSC and CFRP allows the calculation of the compressive force in the HPSC (considering the compressive stress *vs.* strain diagram, which was determined in uniaxial compression and approximated by a bilinear curve given in [25]) and the tensile force in the tendons (considering E_{11} = 180.7 GPa). The determination of the position of the neutral axis c is carried out by iteration of the equilibrium condition of the internal forces. The position of the neutral axis allows now for the calculation of the curvature dφ/dx based on the initially assumed compressive strain on the top edge. The internal moment can thus be calculated from the known compressive stress distribution in the HPSC and the tensile forces in the CFRP tendons. This procedure is repeated by adjusting the compressive strain on the top flange until the internal moment corresponds to the external bending moment, for which one aims to calculate the curvature. Figure 3 shows the comparison of the calculated curvatures following this method with the measured curvatures from the DEMEC readings in the central span of pole No. 7. A good agreement is observed between the calculated and measured curvatures. The pole's failure moment for concrete crushing is then calculated (to $M_{R,calc}$ = 5.71 kNm) following the above procedure and considering a HPSC failure strain on the top flange of 6‰, a value that was experimentally determined in a series of additional flexural tests [25] and which is considerably higher than the usual crushing strains of high strength concretes with other mix designs and compacted by other means [36]. Note that the thus calculated crushing moment of the poles is only 1% lower than the experimentally determined value of $M_{R,exp}$ = 5.76 kNm for pole No. 7 (Figure 3) and 3% higher than the experimentally determined value for pole No. 8.

4.2. Long-Term Bending Behavior Outdoors

The time-dependent load and deformation behavior of the CFRP prestressed HPSC pole Nos. 12–14 (Table 1) is studied in three four-point bending creep tests performed outdoors for 16.5 years. The results presented here describe the specimens' behavior between December 1996, and July 2013. Figure 5 shows the creep deflection at midspan *vs.* time for the three poles loaded at three different load levels. The midspan deflections of the specimens show a rapid increase during the first six months after loading. This is followed by a rather slow increase of deflections, which increase slightly during

the warmer summer months, while they keep stable during the colder part of the year. A possible explanation for this would be the fact that the creep of the HPSC under sustained bending compression and HPSC shrinkage are accelerated by higher temperatures [36].

Figure 4. Quasi-static four-point-bending test of pole No. 8 shortly before failure.

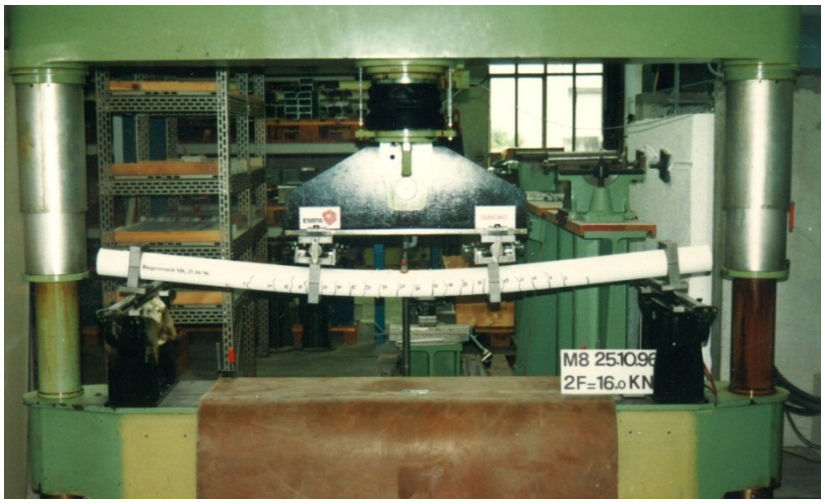

Figure 5. Bending creep tests of pole Nos. 12–14: creep deflection at midspan *vs.* time.

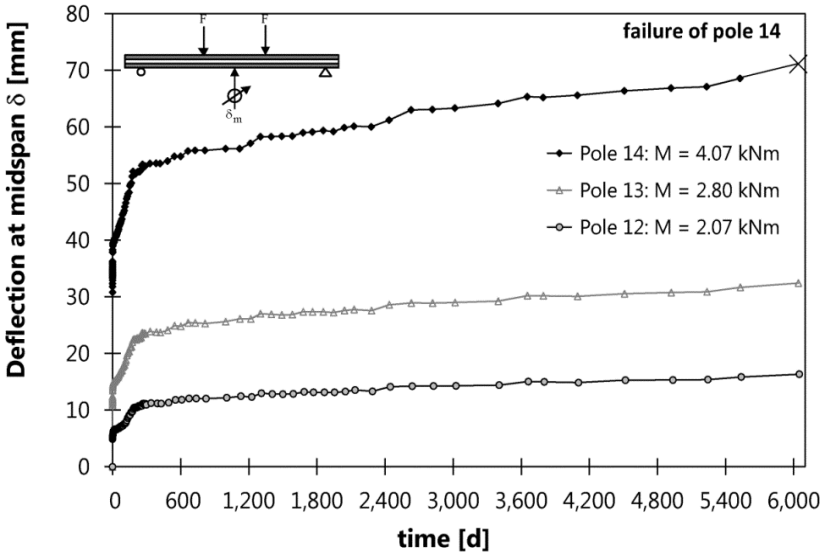

The two less loaded poles, No. 12 (representing a maximum long-term service state) and No. 13, did not fail during the long-term test; both experiments are still running and will be monitored in the years to come. The highest loaded specimen, pole No. 14, sustained a bending moment of 72% of the short-term bending failure moment for 16.5 years before failing 4 July 2013, due to the bond failure of the bottom tendon, which led to local crushing of the HSPC in the ninth crack section located 0.76 m from the northern pole end (Figure 6). The debonding of the Al_2O_3 sand coating from the CFRP tendon surface could be clearly observed at the northern tendon end and by carefully removing the HPSC cover at the tensile edge of the failed cross-section of pole No. 14 (Figure 7, left part of the tendon). Note that this highest loaded CFRP tendon of pole No. 14 (near the tensile edge) was strained to 13.6‰ (2457 MPa) at the beginning of the creep test and that 1.4 years before failure, its strain

increased to 16.28‰ (2942 MPa). This increased tendon stress was calculated from the measured values of $\Delta\varepsilon_{c,max}$ at the top edge and $\Delta\varepsilon_{t,max}$ at the lower edge of the pole and shows the stress redistribution over the section due to bending creep and crack growth. It is hypothesized that this increased bottom tendon strain and the coating's bond creep led to the CFRP anchorage failure by debonding of the Al_2O_3 sand coating from the CFRP tendon surface after 16.5 years.

Figure 6. Failure of pole No. 14 due to slippage of the lowest CFRP tendon in the tensile zone at the north end of the pole, which led to local crushing of the high strength spun concrete.

Figure 7. Detail of the tensile edge of the failed cross-section of pole No.14 after removing the HPSC cover.

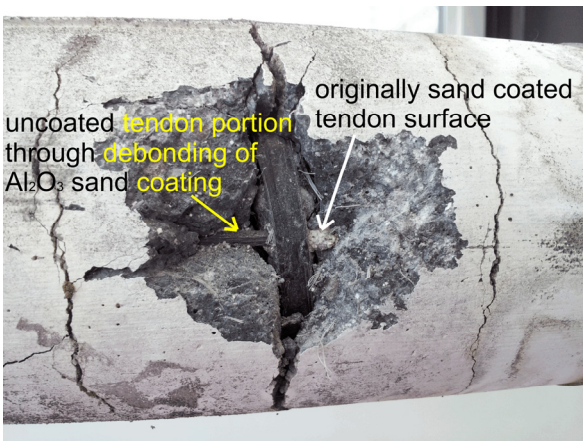

The strain measurements in the central span of the specimens allow calculating the time development of the average bending curvatures, which characterize the long-term bending creep behavior and allow the computation of the bending deflections of the poles. The long-term bending curvatures could be reasonably predicted by a simple analytical model that considers the high strength concrete's compression creep as the deformation controlling mechanism, while as pointed out at the

beginning of Section 4, the prestressed CFRP tendons and the bond thereof to the HPSC are assumed not to creep [25]. This modeling is based on a similar approach as described in [37]. In particular, the controlling creep law for the HPSC was estimated by performing two outdoor compression creep and shrinkage experiments on unreinforced HPSC hollow cylinders of a diameter of 100 mm, a wall thickness of 26 mm (the same cross-section of the poles) and a height of 360 mm for eight months near the bending creep test rigs. For these uniaxial creep experiments, a sustained compressive stress of 50 MPa was applied to the HPSC cylinder specimen after 28 days. This compressive stress corresponds to the average concrete compression stress over the bending compression area of the highest loaded pole No. 14. The creep coefficient φ determined for this test was fitted by logarithmic regression [25] giving:

$$\varphi(t) = 0.5087 \times \ln(t) - 0.1874 \ (t \text{ in days}) \tag{1}$$

The total compressive creep strain of the HPSC $\varepsilon_c(t)$ is then calculated as a function of the time t under sustained load:

$$\varepsilon_c(t) = \varepsilon_c(t = 0) \times [1 + \varphi(t)] \ (t \text{ in days}) \tag{2}$$

The effects of creep can be approximated by reducing the modulus of elasticity of the HPSC $E_c(\varepsilon_c)$, measured for short-term loading [35]:

$$\begin{gathered} E_c(\varepsilon_c, t) = \frac{E_c(\varepsilon_c)}{1+\varphi(t)} \text{ with } E_c(\varepsilon_c) = 35{,}000 \text{ MPa for } |\varepsilon_c| < 2.38‰ \\ E_c(\varepsilon_c) = 5710 + \frac{69.63}{\varepsilon_c} \text{ MPa for } 2.38‰ < |\varepsilon_c| < 6‰ \end{gathered} \tag{3}$$

where $E_c(\varepsilon_c)$ is derived from a bilinear compression stress-strain relationship determined in [25].

In the uncracked state, both the tensile and compressive zone creep under the long-term bending moment; this causes a steady curvature increase. For modeling the curvature increase with time, the assumption was made that the HPSC shows the same creep behavior under tensile and compressive stress, which is described with Equation (3). Note that the strains of the uncracked HPSC are limited by its tensile strength of 10.9 MPa; therefore, the elastic modulus of the uncracked HPSC is assumed to be independent of the strain. The calculation of the increase of the bending creep curvature of the uncracked HPSC section is now straightforward and requires determining the ideal moment of inertia I of the full cross-section and the consideration of the creep modulus of the HPSC given in Equation (3):

$$\frac{d\varphi(t)}{dx} = \frac{M}{I \cdot E_c(\varepsilon_c, t)} \ (t \text{ in days}) \tag{4}$$

Figure 8 shows the experimental bending curvature *vs.* time for pole No. 12, which is initially uncracked for six months, and the bending creep curvature approximation with the model described, which overestimates the measured creep curvature during this first six months. Even after first very thin bending cracks appear, the analytically calculated curvature is overestimating the experimental curvature. For the cracked poles (pole No. 12 after six months; pole Nos. 13 and 14 from the beginning of the creep tests), predominantly, the concrete compression zone creeps under the long-term load, while the load bearing capacity of the concrete in the tensile zone is neglected. In [37], a model to calculate long-term bending curvatures was developed for a concrete-GFRP-CFRP hybrid beam. The

authors assumed that shrinkage and creep of the hybrid beam components can be modeled by strain and stress redistribution to satisfy the equilibrium and kinematic compatibility conditions. A similar type of direct analysis is performed in the present study. For a given loading time t an initial value of the HPSC strain at the compressive edge $\varepsilon_c(t, r_a)$ is assumed. The elastic modulus of the HPSC after t is then estimated with Equation (3) under consideration of the creep coefficient given by Equation (1). These parameters allow the calculation of the strain-plane of the prestressed cylindrical cross-section under consideration of the force equilibrium condition, of the kinematic conditions of the slender beam and of the stress-strain relationships of CFRP and HPSC (3) under the assumption of the absence of bond creep. In particular, the cross-section analysis considered that the prestressed tendons in the compressive zone have a tensile pre-strain that is reduced by the flexural bending strain. All tendon forces (*i.e.*, also for the tendons in the compressive zone) are taken into account in the section's equilibrium of internal compression (in the concrete) and tension force. The iteration of $\varepsilon_c(t, r_a)$ till equilibrium of the internal moment with the (external) bending creep moment is reached, provides the desired strain-plane of the cross-section after loading time t. During iteration, the failure strains of CFRP (21‰) and HPSC compressive edge (−6‰) are checked for. In accordance with [37], the assumption is made that the failure strains of CFRP and HPSC are independent of the creep time. The bending creep curvatures of poles Nos. 13 and 14 estimated following this procedure are compared with the experimentally determined curvatures in Figure 8. The calculated curvatures show a reasonably good agreement with the experimental ones. The high curvature after one year of sustained creep is shown in Figure 2 for the highest loaded pole, No. 14. Note that the rate of creep is initially lower (for the first six months) and subsequently higher than observed in practice. This is explained with the influence of the climate: the outdoor creep tests were started at the beginning of a hard winter, during which, temperatures stayed between −10 °C and +15 °C. This fact led to a low creep rate during the first six months of testing. With the higher summer temperatures after that (20 °C to 35 °C), the creep rate increased in the next six months. From the second testing year on, the creep deflection under sustained bending loads increased always during the warmer summer months.

Figure 8. Bending creep curvatures *vs.* time for pole Nos. 12–14 (16.5 years of monitoring).

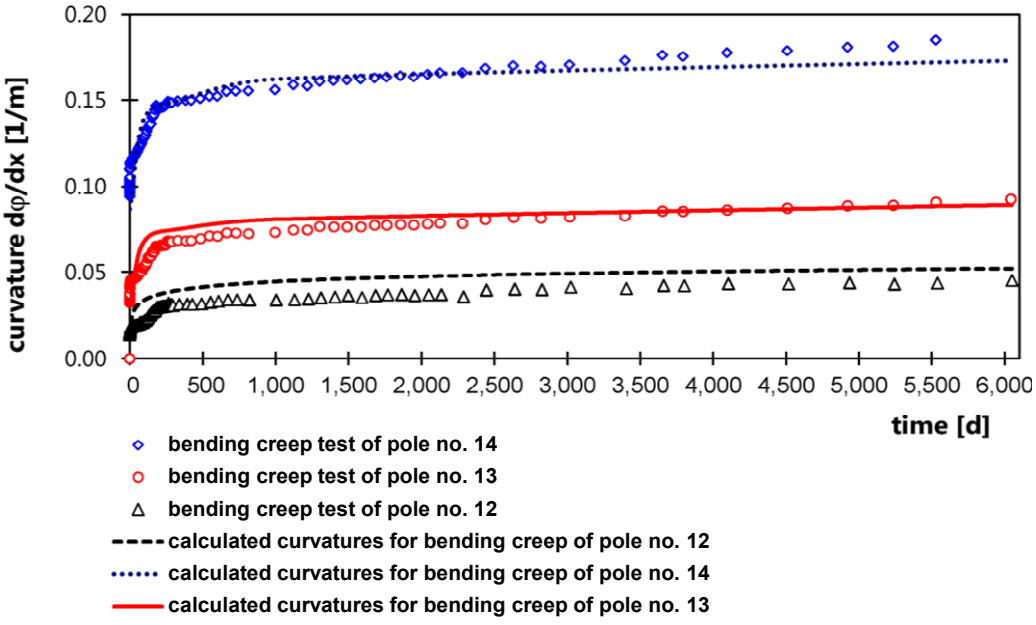

Slippage monitoring for the top and bottom CFRP tendon ends of poles Nos. 12 and 13 (next to the poles' compressive and tensile edge, respectively) showed a limited draw-in of the tendons between 0.8 mm and 1.6 mm (top tendons) and from 0.8–1.1 mm (bottom tendons) in 16.5 years. It is hypothesized that one part of these slippages is an artifact caused by the erosion of the epoxy matrix of the tendons' free ends by UV radiation. This was confirmed by optical microscope analysis of the free tendon ends, which showed clear erosion after 16.5 years. Therefore, the effective draw-in of the highest tension-loaded (bottom) tendons is assumed to be considerably lower than the measured 0.8–1.1 mm. This limited tendon slippage is the proof for the long-term durability of the bond between HPSC and CFRP in mid-European climatic conditions, achieved through Al_2O_3 sand coating of the CFRP surface: bond creep at the HPSC/CFRP interface is thus very limited over 16.5 years. Note that the bending creep moment applied to pole No. 12 represents a maximum long-term design bending load state [33]. This result confirms the above hypothesis that creep and shrinkage of the HPSC are controlling the long-term deformations of the pole specimens.

Figure 9. Development of the number of cracks and crack widths of the highest loaded pole, No. 14.

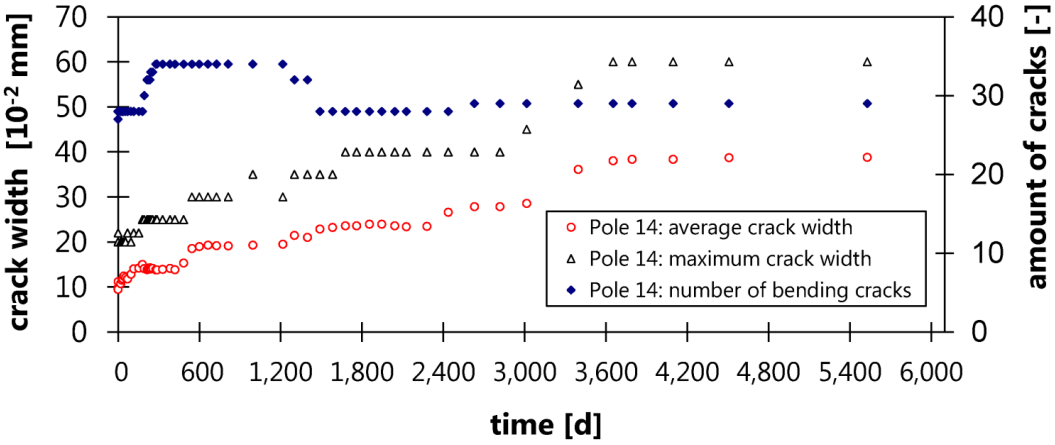

Crack positions and crack widths were recorded for poles Nos. 13 and 14 during the long-term creep tests, and the crack amounts and widths recorded over 15 years are exemplary shown for pole No. 14 in Figure 9: the number of cracks stabilizes after one year of testing and even decreases after 3.5 years, because some thinner cracks close under prestress, due to the cement hydration continuing over years (HPSC cement content is 600 kg·m^{-3}), while a slight increase in average and maximum crack widths occurs with increasing time, reaching end values of 0.4 mm and 0.6 mm, respectively. Pole No. 12, which was loaded with over 80% of the short-term cracking moment, shows 10 very thin bending cracks (width 0.02 mm) after six months of testing. Six months later, the amount of thin cracks has increased to 17, a number that has been constant for the following 15.5 years. Note that the tensile edge of pole No. 12 is subjected to an initial bending stress of 8.8 MPa, which is very near to the average tensile strength of 10.9 MPa for the HPSC determined in three-point bending tests at 28 days.

5. Conclusions

The long-term behavior of a series of highly loaded CFRP prestressed spun concrete pole specimens was presented in this study. The poles have been subjected to outdoor four-point bending

creep tests at EMPA since 1996 in the frame of collaboration with the Swiss precast concrete producer, SACAC. The 2-m span cylindrical beams studied are models for lighting poles produced for the last 10 years and sold on the European market. Five thin-walled pole specimens were investigated (diameter: 100 mm; wall-thickness: 25–27 mm). All specimens had been produced in a pretensioning and spinning technique and were prestressed by eight Ø3 mm pultruded CFRP tendons. The sand-coated CFRP prestressing tendons were subjected to an initial prestress of 47% of their average tensile strength of 3375 MPa. Initially, two reference pole specimens were tested in quasi-static, four-point bending to determine the short-term failure moment and to model the short-term flexural behavior. Then, three pole specimens (Nos. 12–14) were loaded with three different sustained bending creep moments, and the tests were run for 16.5 years. The following conclusions can be drawn on the basis of the study described in this paper:

1. The short-term bending behavior of CFRP prestressed HPSC poles is bilinear with considerable rotation capacity at failure. The moment *vs.* curvature behavior and the failure moment for HPSC crushing can be modeled by a simple cross-sectional analysis following the beam theory of hybrid prestressed cross-sections.
2. The long-term bending serviceability of CFRP prestressed HPSC poles is satisfactory for realistic service moments, represented by the lowest loaded pole, No. 12, in the test series presented. Long-term curvatures and deflections stabilize after six months of sustained loading. Furthermore, pole specimens under realistic long-term service moments showed crack patterns that were stable over time and minimal slippage of the tendons with respect to the pole's end faces. The latter proves the successful and durable anchorage of the Al_2O_3 sand-coated CFRP prestressing tendons of this study in thin-walled precast concrete members under realistic long-term service loads.
3. Pole No. 14, which was loaded with twice the maximum long-term service moment, failed after 16.5 years, due to bond failure of the highest loaded CFRP tendon. The debonding of the Al_2O_3 sand coating from the CFRP tendon surface could be clearly observed.
4. The long-term evolution of curvatures due to bending creep of the poles could be modeled analytically with reasonable accuracy using a simple, direct analysis based on the assumption that HPSC creep governs the strain and stress redistribution over the cross-section with time.

Acknowledgments

The authors would like to thank SACAC Schleuderbetonwerk AG and, in particular, its former managing director, Mr. Georges Bättig, for their collaboration in the fruitful development works over the last 20 years. The valuable support regarding testing matters by Mr. Heinrich Lippuner und Mr. Bruno Maag of the Structural Engineering Laboratory of EMPA was also greatly appreciated. The Head of the Structural Engineering Laboratory, Prof. Dr. Masoud Motavalli, is acknowledged for his steady support with the long-term monitoring over the past 17 years. This project was partially funded by the Commission for Technology and Innovation (CTI) of the Swiss Confederation.

Author Contributions

Giovanni P. Terrasi was responsible for the design, for the innovative technology development of CFRP prestressed HPSC, for the specimen production and for defining and performing the experiments described in the paper and for the test data evaluation and analysis. Christian Affolter worked on the short- and long-term mechanical numerical and analytical modelling, such as on materials characterization. Urs Meier initiated the project and was involved in intensive discussions about the result analysis and visco-elastic modelling. All authors were of course involved in the manuscript preparation and in an in depth literature analysis.

Conflicts of Interest

The authors declare no conflict of interest.

References

1. Gerritse, A.; Schürhoff, H.J. Prestressing with Aramid Tendons. In Proceedings of the 10th FIP Congress, New Delhi, India, 16–20 February 1986.
2. Rostásy, F.S.; Budelmann, H. High strength fiber composites for prestressing. *Mater. Eng.* **1990**, *3*, 779–792.
3. Lees, J.M.; Burgoyne, C.J. Experimental study of influence of bond on flexural behavior of concrete beams pretensioned with aramid fiber reinforced plastics. *ACI Struct. J.* **1999**, *96*, 377–385.
4. Lees, J.M.; Burgoyne, C.J. Transfer bond stresses generated between FRP tendons and concrete. *Mag. Concr. Res.* **1999**, *51*, 229–239.
5. Sen, R.; Shahawy, M.; Sukumar, S.; Rosas, J. Durability of carbon fiber reinforced polymer (CFRP) pretensioned elements under tidal/thermal cycles. *ACI Struct. J.* **1999**, *96*, 450–457.
6. Nanni, A.; Tanigaki, M. Pretensioned prestressed concrete members with bonded fiber reinforced plastic tendons: development and flexural bond lengths (static). *ACI Struct. J.* **1992**, *89*, 433–441.
7. Terrasi, G.P.; Bättig, G.; Brönnimann, R. Pylons made of high-strength spun concrete and prestressed with carbon fibre reinforced plastic for high power transmission lines. *Int. J. Matter. Prod. Technol.* **2002**, *17*, 32–45.
8. Portnov, G.; Bakis, C.E.; Lackey, E.; Kulakov, V. FRP Reinforcing bars designs and methods of manufacture (Review of Patents). *Mech. Compos. Mater.* **2013**, *49*, 1–20.
9. Sayed Ahmad, F.; Foret, G.; Le Roy, R. Bond between carbon fibre-reinforced polymer (CFRP) bars and ultra high performance fibre reinforced concrete (UHPFRC): Experimental study. *Constr. Build. Mater.* **2011**, *25*, 479–485.
10. Nanni, A.; Bakis, C.E.; O'Neil, E.F.; Dixon, T.O. Performance of FRP tendon-anchor systems for prestressed concrete structures. *PCI J.* **1996**, *41*, 34–44.
11. Toutanji, H.; Saafi, M. Performance of concrete beams prestressed with aramid fiber-reinforced polymer tendons. *Compos. Struct.* **1999**, *44*, 63–70.

12. Campbell, T.I.; Shrive, N.G.; Soudki, K.A.; Al-Mayah, A.; Keatley, J.P.; Reda, M.M. Design and evaluation of a wedge-type anchor for fibre reinforced polymer tendons. *Ca. J. Civil Eng.* **2000**, *27*, 985–992.
13. Cosenza, E.; Manfredi, G.; Realfonzo, R. Behavior and modeling of bond of FRP rebars to concrete. *J. Compos. Constr.* **1997**, *1*, 40–51.
14. De Lorenzis, L.; Miller, B.; Nanni, A. Bond of fiber-reinforced polymer laminates to concrete. *ACI Mater. J.* **2001**, *98*, 256–264.
15. Bakis, C.E.; Uppuluri, V.S.; Nanni, A.; Boothby, T.E. Analysis of bonding mechanisms of smooth and lugged frp rods embedded in concrete. *Compos. Sci. Technol.* **1998**, *58*, 1307–1319.
16. Mahmoud, Z.I.; Rizkalla, S.H. Bond of CFRP prestressing reinforcement. In Proceedings of 2nd International Conference on Advanced Composite Materials in Bridges and Structures, Montreal, Canada, 11–14 August 1996.
17. Gerritse, A.; Den Uijl, J. Long term behaviour of arapree. In Proceedings of Non-Metallic (FRP) Reinforcement for Concrete Structures (FRPRCS-2), Ghent, Belgium, 23–25 August 1995; pp. 57–66.
18. Shahidi, F. Bond degradation between FRP bars and concrete under sustained loads. Ph.D. Thesis, University of Saskatchewan, Saskatoon, Canada, 2003.
19. Fornůsek, J.; Konvalinka, P.; Sovják, R.; Vítek, J.L. Long-term behaviour of concrete structures reinforced with pre-stressed GFRP tendons. *WIT Trans. Model. Simul.* **2009**, *1*, 535–545.
20. Terrasi, G.P.; Brönnimann, R.; Bättig, G. CFRP tendon prestress monitoring by resistance measurement in a spun concrete powerline pylon. In Proceedings of the first middle east conference on smart monitoring, assessment and rehabilitation of civil structures (SMAR 2011), American University, Dubai, UAE, 8–10 February 2011.
21. Zou, P.X.W. Long-term deflection and cracking behavior of concrete beams prestressed with carbon fiber-reinforced polymer tendons. *J. Compos. Constr.* **2003**, *7*, 187–193.
22. Zou, P.X.W.; Shang, S. Time-dependent behaviour of concrete beams pretensioned by carbon fibre-reinforced polymers (CFRP) tendons. *Constr. Build. Mater.* **2007**, *21*, 777–788.
23. Youakim, S.A.; Karbhari, V.M. An approach to determine long-term behavior of concrete members prestressed with FRP tendons. *Constr. Build. Mater.* **2007**, *21*, 1052–1060.
24. Rodriguez-Gutierrez, J.A.; Aristizabal-Ochoa, J.D. Short- and long-term deflections in reinforced, prestressed, and composite concrete beams. *J. Struct. Eng.* **2007**, *133*, 495–506.
25. Terrasi, G.P. Mit Kohlenstoffasern vorgespannte Schleuderbetonrohre. Ph.D. Thesis, Eidgenössische Technische Hochschule (ETH), Zurich, Switzerland, 1998. (In German)
26. Agyei, B.B.; Lees, J.M.; Terrasi, G.P. Fatigue of high strength concrete beams pretensioned with CFRP tendons. In Proceedings of 6th International Symposium on Fibre-Reinforced Polymer (FRP) Reinforcement for Concrete Structures (FRPRCS-6), Singapore, 8–10 July 2003.
27. Roberts, E.E.; Lees, J.M.; Hoult, N.A. Flexural fatigue performance of CFRP prestressed concrete poles. *Adv. Struct. Eng.* **2012**, *15*, 575–588.
28. Uomoto, T. Durability considerations of FRP reinforcement. In Proceedings of the Non-Metallic (FRP) Reinforcement for Concrete Structures (FRPRCS-5), Cambridge, UK, 16–18 July 2001.

29. Burgoyne, C.J. Rational use of advanced composites in concrete. In Proceedings of the Non-Metallic (FRP) Reinforcement for Concrete Structures (FRPRCS-3), Sapporo, Japan, 14–16 October 1997.
30. Terrasi, G.P. Prefabricated Thin-walled Structural Elements Made from High Performance Concrete Prestressed with CFRP Wires. *J. Mater. Sci. Res.* **2013**, *2*, doi:10.5539/jmsr.v2n1p1.
31. Terrasi, G.P.; Lees, J.M. CFRP Prestressed Concrete Lighting Columns. *Am. Concr. Inst. Int.* **2003**, *215*, 55–74.
32. American Concrete Institute (ACI). *Prestressing Concrete Structures with FRP Tendons*, ACI 440. 4R-04; Detroit, MI, USA, 2004.
33. Swiss Standard. *SN 505 160, Loads on Structures*, SIA 160; Swiss Engineers and Architects Society, Zurich, Switzerland, 1989.
34. Saadatmanesh, H.; Tannous, F.E. Relaxation, creep, and fatigue behavior of carbon fiber reinforced plastic tendons. *ACI Mater. J.* **1999**, *96*, 143–153.
35. Bachmann, H. *Spannbeton II (Prestressed Concrete);* Vdf university publishers of ETH (Eidgenössische Technische Hochschule): Zurich, Switzerland, 1991. (In German)
36. Held, M. A Contribution to the Production and Design of Compressive Members made of High Strength Concrete. Ph.D. Thesis, Technische Universität Darmstadt, Darmstadt, Germany, 1992.
37. Deskovic, N.; Meier, U.; Triantafillou, T.C. Innovative design of FRP combined with concrete: Long-term behavior. *J. Struct. Eng. NY* **1995**, *121*, 1079–1089.